

SUPPORTING INFORMATION

Sub-100-nanometer Silver Doped Gold-Cysteine Supramolecular Assemblies with Enhanced Nonlinear Optical Properties

*Hussein Fakhouri,¹ Martina Perić,² Franck Bertorelle,¹ Philippe Dugourd,¹ Xavier Dagany,¹
Isabelle Russier-Antoine,¹ Pierre-François Brevet,¹ Vlasta Bonačić-Koutecký,^{2,3} and
Rodolphe Antoine^{1*}*

¹Univ Lyon, Université Claude Bernard Lyon 1, CNRS, Institut Lumière Matière, UMR5306, Lyon, France

²Center of Excellence for Science and Technology-Integration of Mediterranean Region (STIM) at Interdisciplinary Center for Advanced Sciences and Technology (ICAST), University of Split, Poljička cesta 35, 21000 Split, (Croatia)

³Chemistry Department, Humboldt University of Berlin, Brook-Taylor-Strasse 2, 12489 Berlin (Germany), vbk@chemie.hu-berlin.de

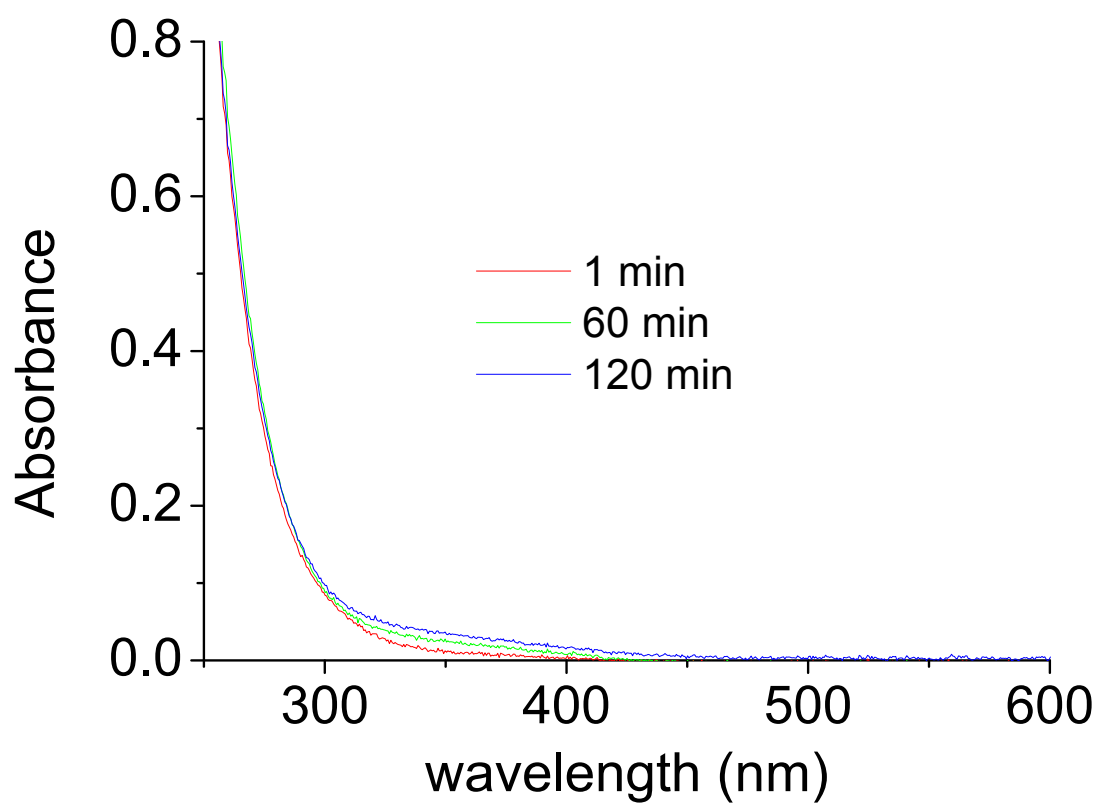


Figure S1 : UV-Vis absorption spectra of polymeric species of $-[\text{Cys-Au(I)}]_n-$ produced in the first step at high pH and in presence of TEA, at different times.

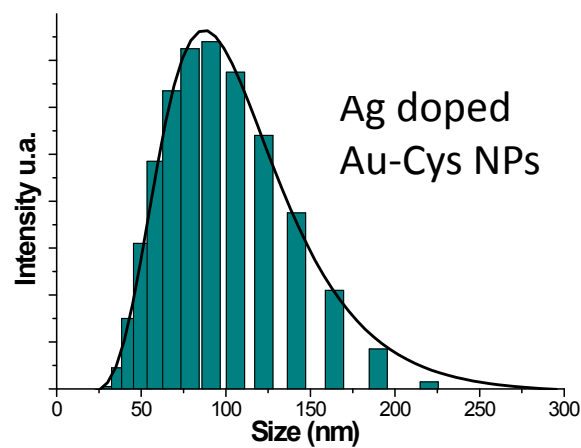
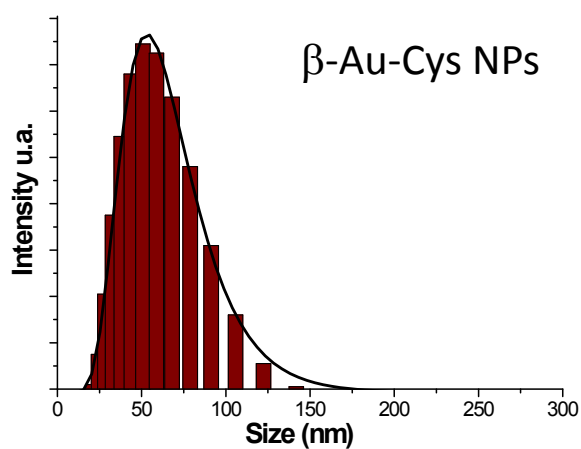
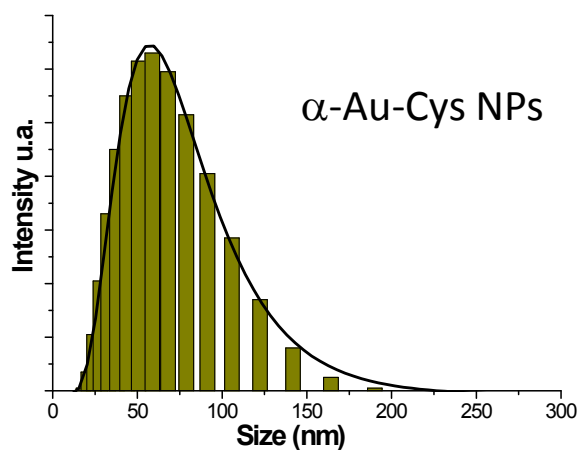


Figure S2 : size distributions for α -Au-Cys, β -Au-Cys, and Ag-doped Au-Cys NPs in aqueous solutions obtained by dynamic light scattering (DLS). Experimental distributions are fitted with lognormal distributions. The corresponding full widths at half maximum are 50, 40 and 66 nm for α -Au-Cys, β -Au-Cys, and Ag-doped Au-Cys NPs respectively.

Table S1 : Quantitative XPS results of typical NPs samples spectra which has been recorded in order to determine the effect of X-ray irradiation on the chemical state of the sample.

	C	O	Au	N	S	Ag
α -Au-Cys NPs (% content)	37.6	24.4	13.4	14.0	10.8	--
β -Au-Cys NPs (% content)	37.8	23.8	14.5	13.0	11.0	--
Ag-doped Au-Cys NPs (% content)	35.1	23.7	15.3	13.0	10.8	1.5

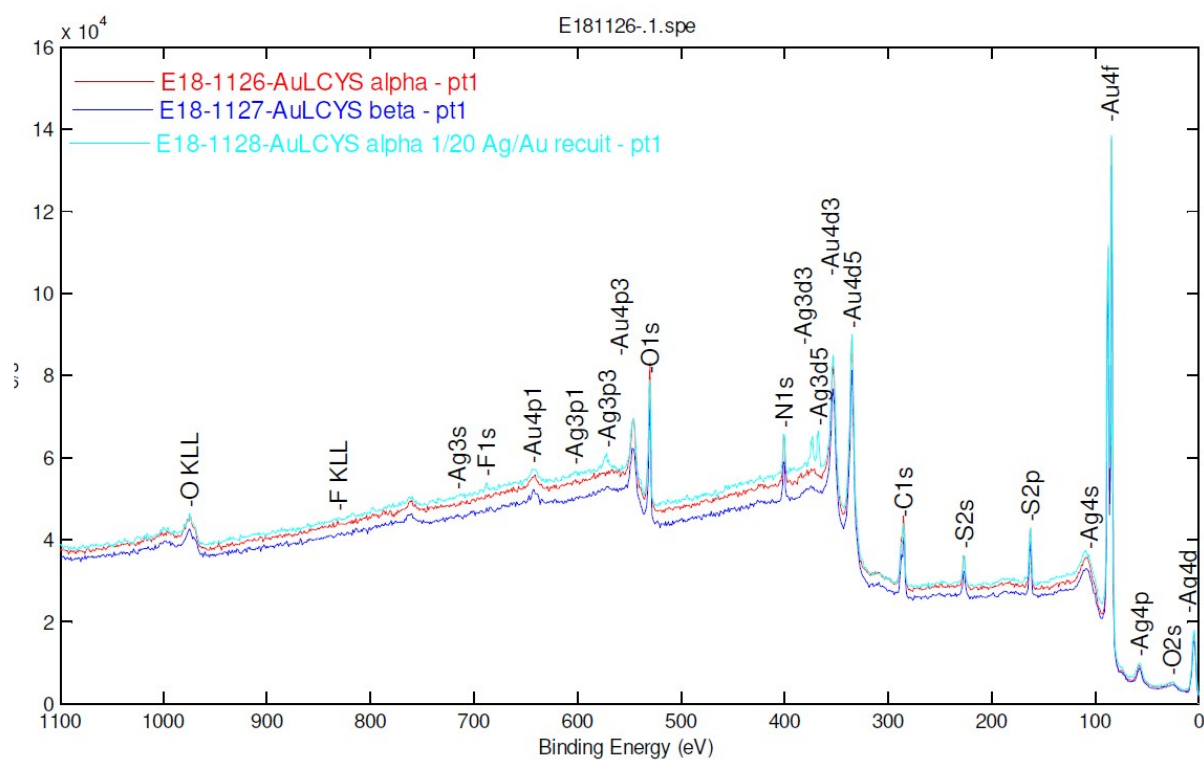


Figure S3 : XPS results showing spectra of all chemical element composition for α -Au-Cys, β -Au-Cys, and Ag-doped Au-Cys NPs.

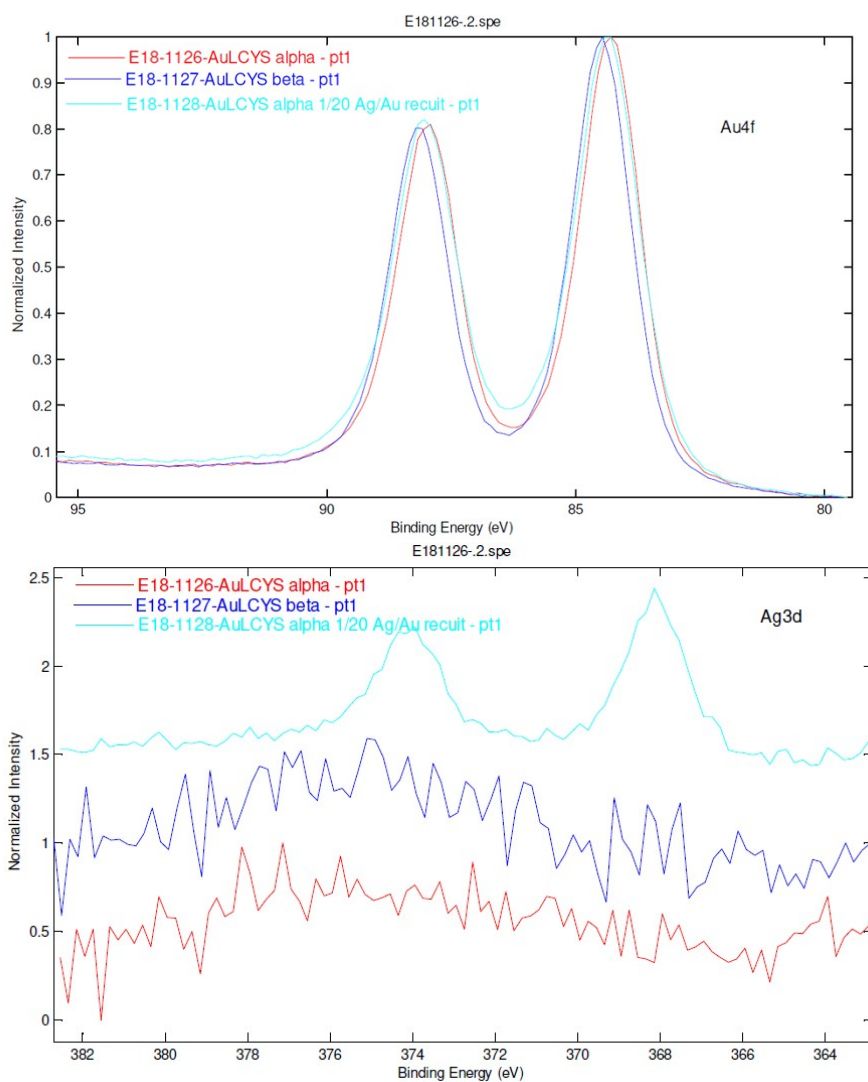


Figure S4 : (top) Au 4f binding energy (BE) of the α -Au-Cys (red), β -Au-Cys (blue), and Ag-doped Au-Cys (cyan) NPs. (bottom) Ag 3d binding energy (BE) of the α -Au-Cys (red), β -Au-Cys (blue), and Ag-doped Au-Cys (cyan) NPs.

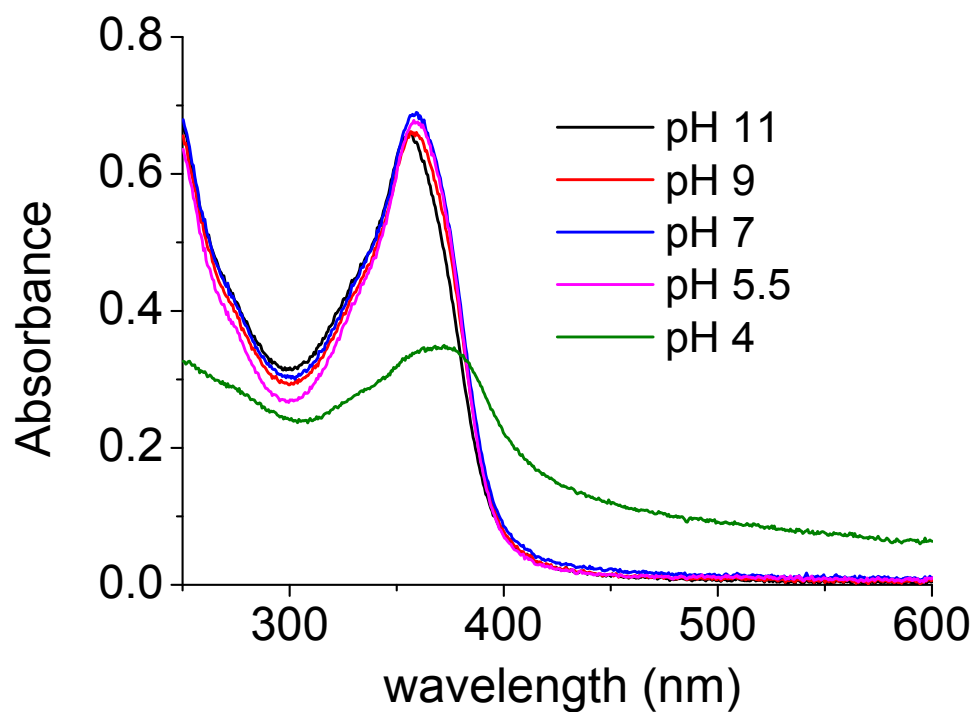


Figure S5 : UV-Vis absorption spectra of α -Au-Cys NPs after 3 days under agitation as a function of pH (HCl/TEA was used for pH controlled experiments and the pH was measured with a pHmeter).

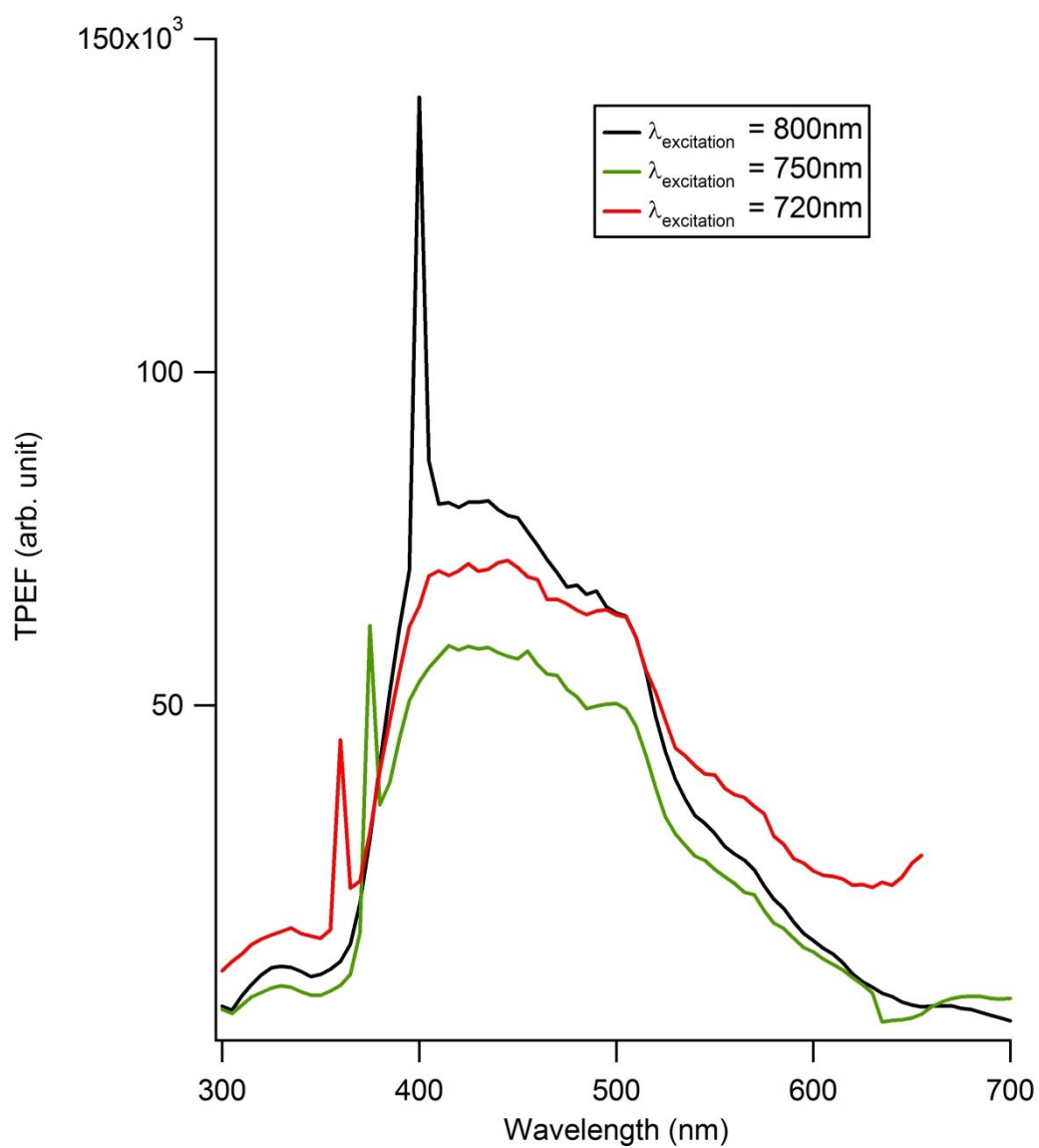


Figure S6 : TPEF spectra of Ag-doped Au-Cys NPs aqueous solution (NPs concentration of 0.1 nM) at three different excitation wavelength, namely 720, 750 and 800 nm. The hyper Rayleigh band is also visible at half the excitation wavelength.

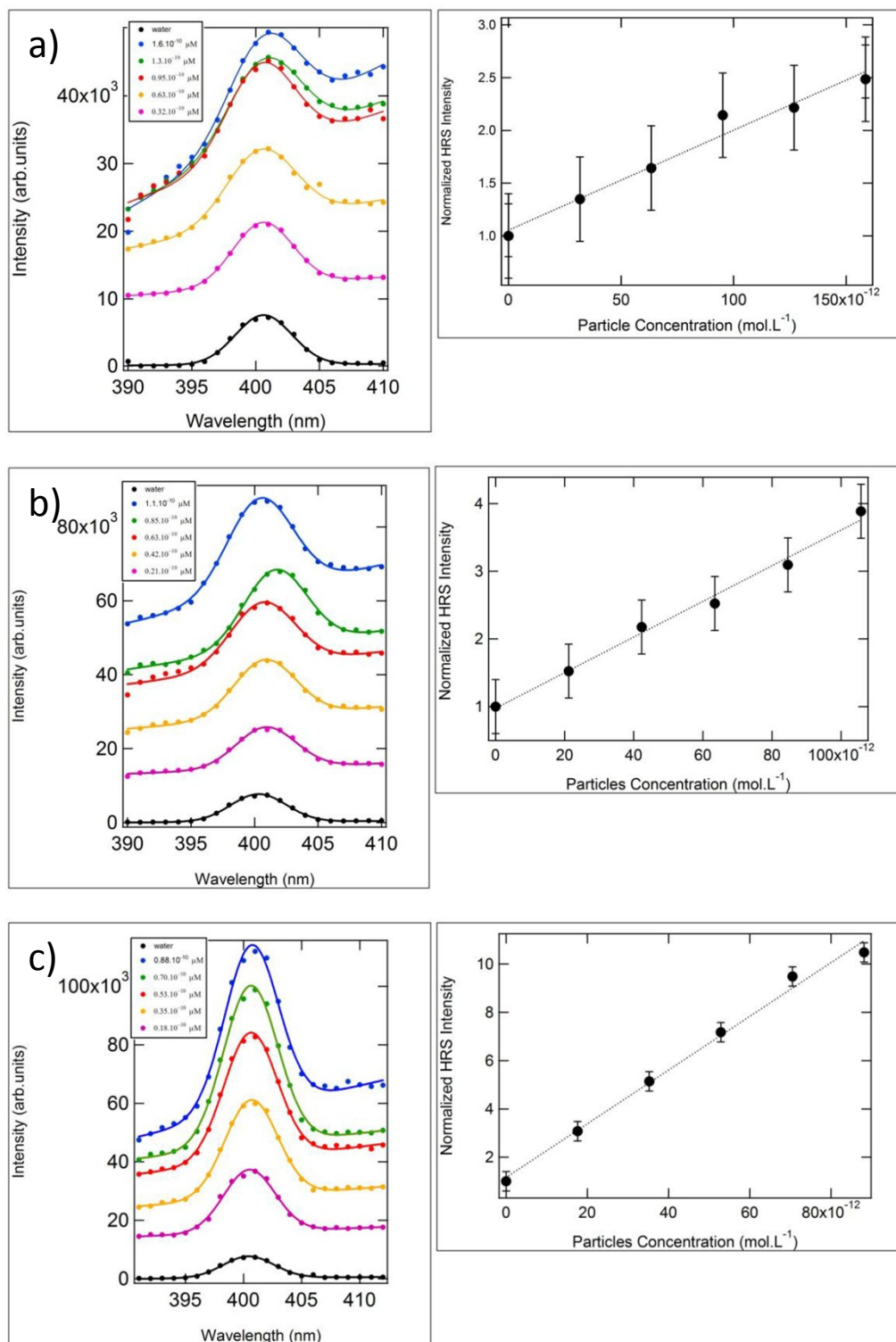


Figure S7 : (left panels) HRS line intensity for supramolecular NPs in aqueous solutions for different concentrations. Line: fit to a Gaussian function superposed on a linearly increasing function of the wavelength accounting for the broadband multiphoton excited emission. (right panels). Plot of the HRS intensity as extracted from the right hand-side panels for the supramolecular NPs in aqueous solution as a function of concentration. The continuous line corresponds to a linear fit. a) α -Au-Cys, b) β -Au-Cys, and c) Ag-doped Au-Cys NPs.

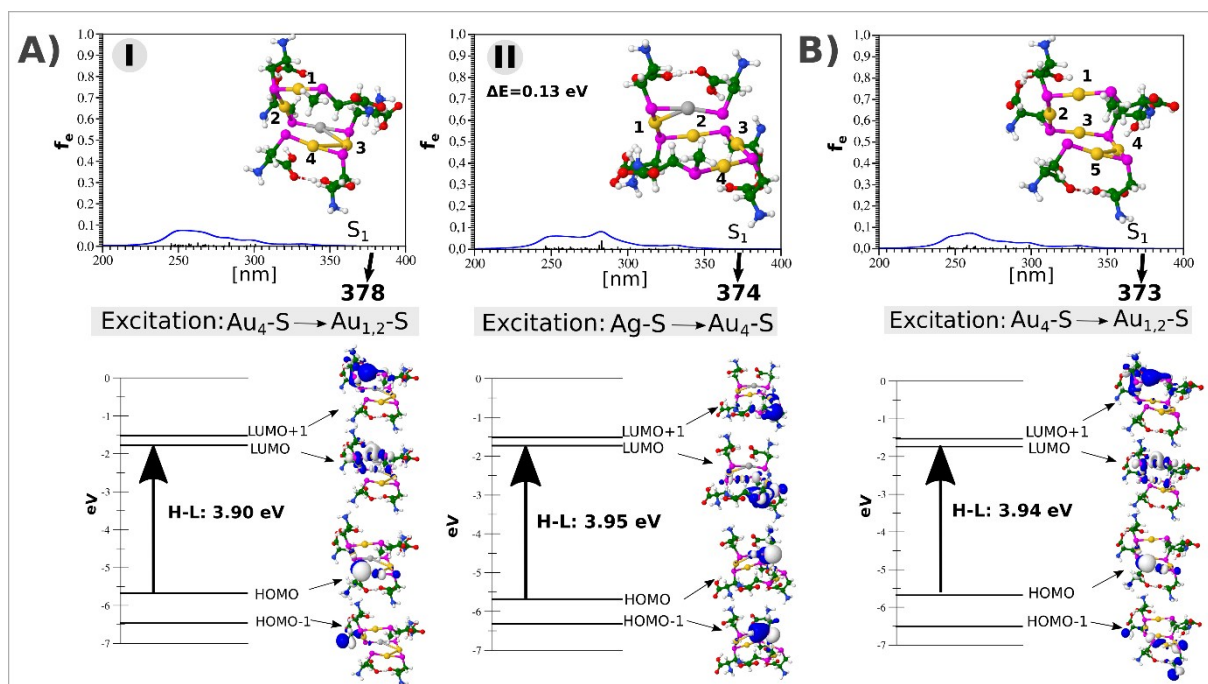


Figure S8 : (upper part) TDDFT OPA spectra for optimized structures A) Au₄-Ag-Cys₆-CH₃ (isomers I and II) and B) Au₅-Cys₆-CH₃. The structures involved in the leading excitations to the S₁ state are given on the absorption spectra. (lower part) Energies and analysis of the Molecular Orbitals. Broadening of the lines is simulated with a Lorentzian profile with half-width of 15 nm (blue lines). Metallic bond lengths of optimized dimers structures are substantially elongated in comparison with bond lengths of corresponding dimers.

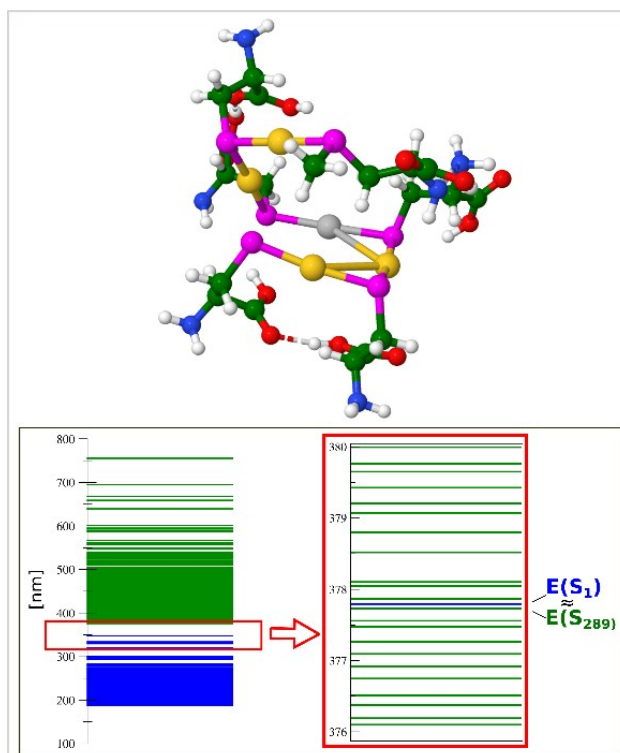


Figure S9: Energies of one-photon OPA (blue) and two-photon TPA (green) states in nm illustrating the resonance between S_1 OPA and S_{289} TPA excited states of $Au_4-Ag-Cys_6-CH_3$.

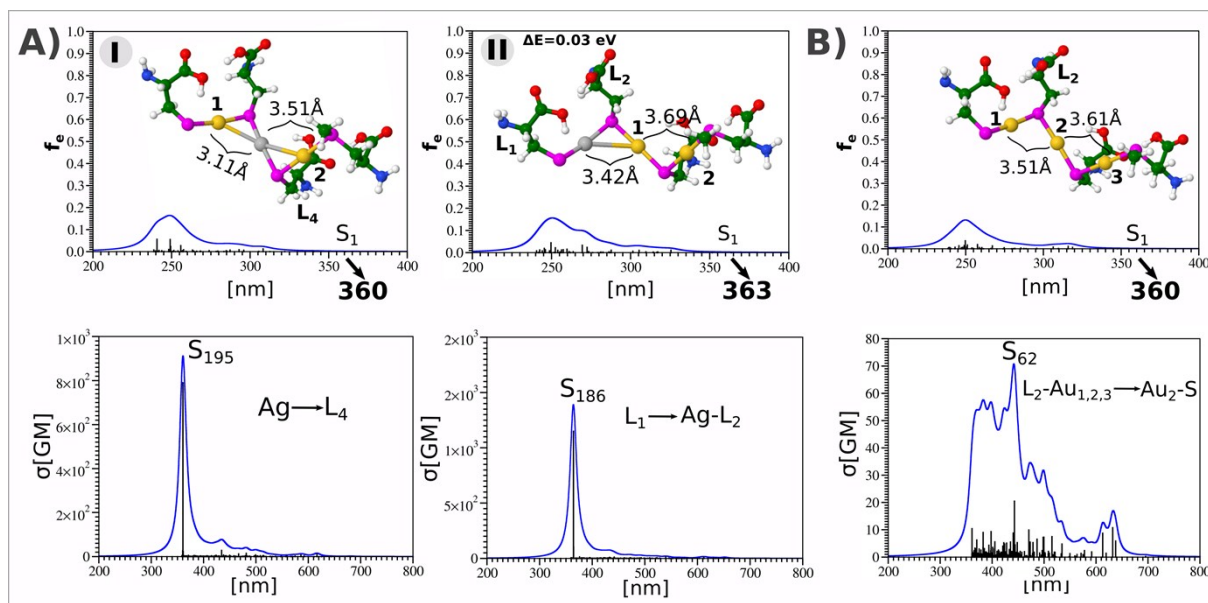


Figure S10: TDDFT (upper part) OPA and (lower part) TPA spectra for optimized structures of model system: A) $Au_2-Ag-Cys_4-CH_3$ (isomers I and II) and B) $Au_3-Cys_4-CH_3$. Parts of structures involved in leading excitation of S_{195} , S_{186} and S_{62} states are labeled according to structures shown in upper part. Broadening of the lines is simulated by the Lorentzian function with half-width of 15 nm (blue lines).

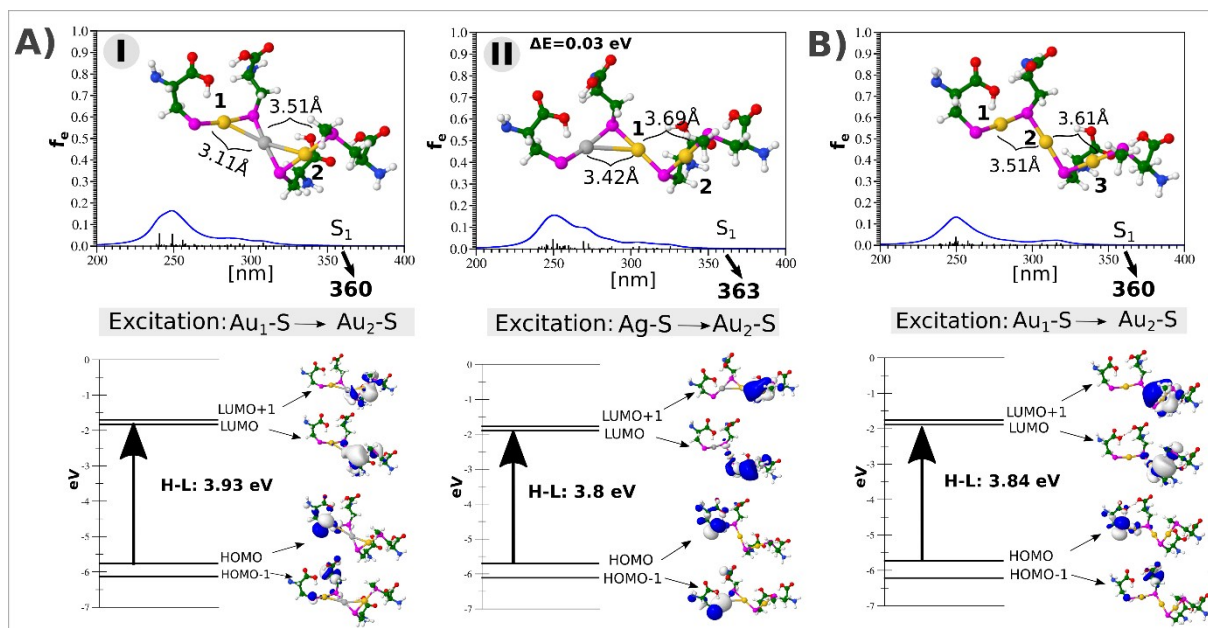


Figure S11: TDDFT OPA spectra for shown optimized structures A) Au₂-Ag-Cys₄-CH₃ (isomers I and II) and B) Au₃-Cys₄-CH₃. Parts of structures involved in leading excitations for S₁ state are given below OPA spectra (upper part). Energies and analysis of MO's (lower part). Broadening of the lines is simulated by the Lorentzian function with half-width of 15 nm (blue lines).

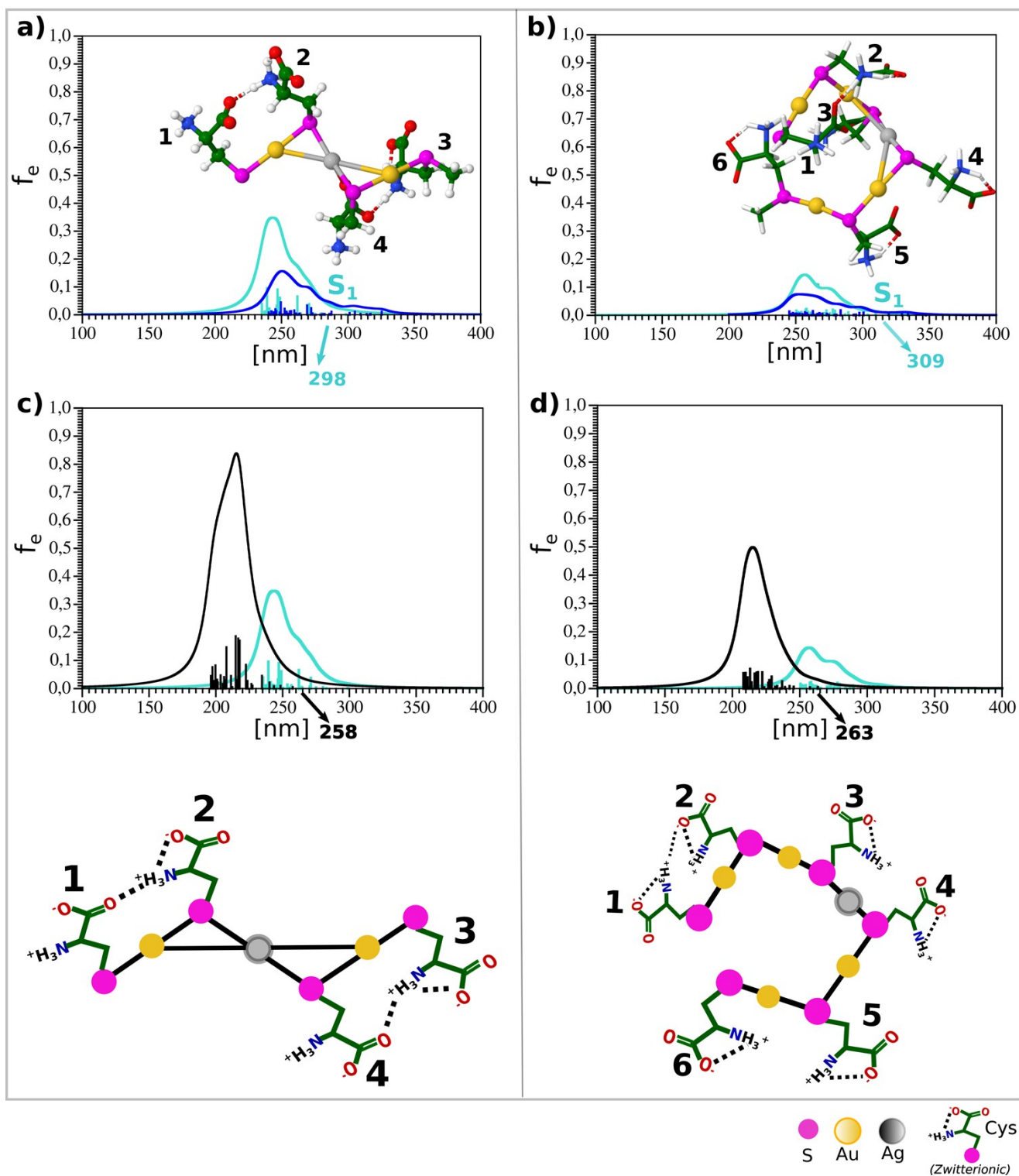


Figure S12: Comparison of OPA spectra obtained for optimized structures of two model systems a) Au₂-Ag-Cys₄-CH₃ and b) Au₄-Ag-Cys₆-CH₃ in gas phase (blue) and in water (turquoise) using TDDFT with B3LYP functional and SMD approach for solvent. Comparison of functional CAM-B3LYP (black) with B3LYP (turquoise) of OPA spectra, c) and d), for two model systems including solvent with SMD approach. Schematic illustration of interacting cysteine pairs within solvent is shown in lower part.

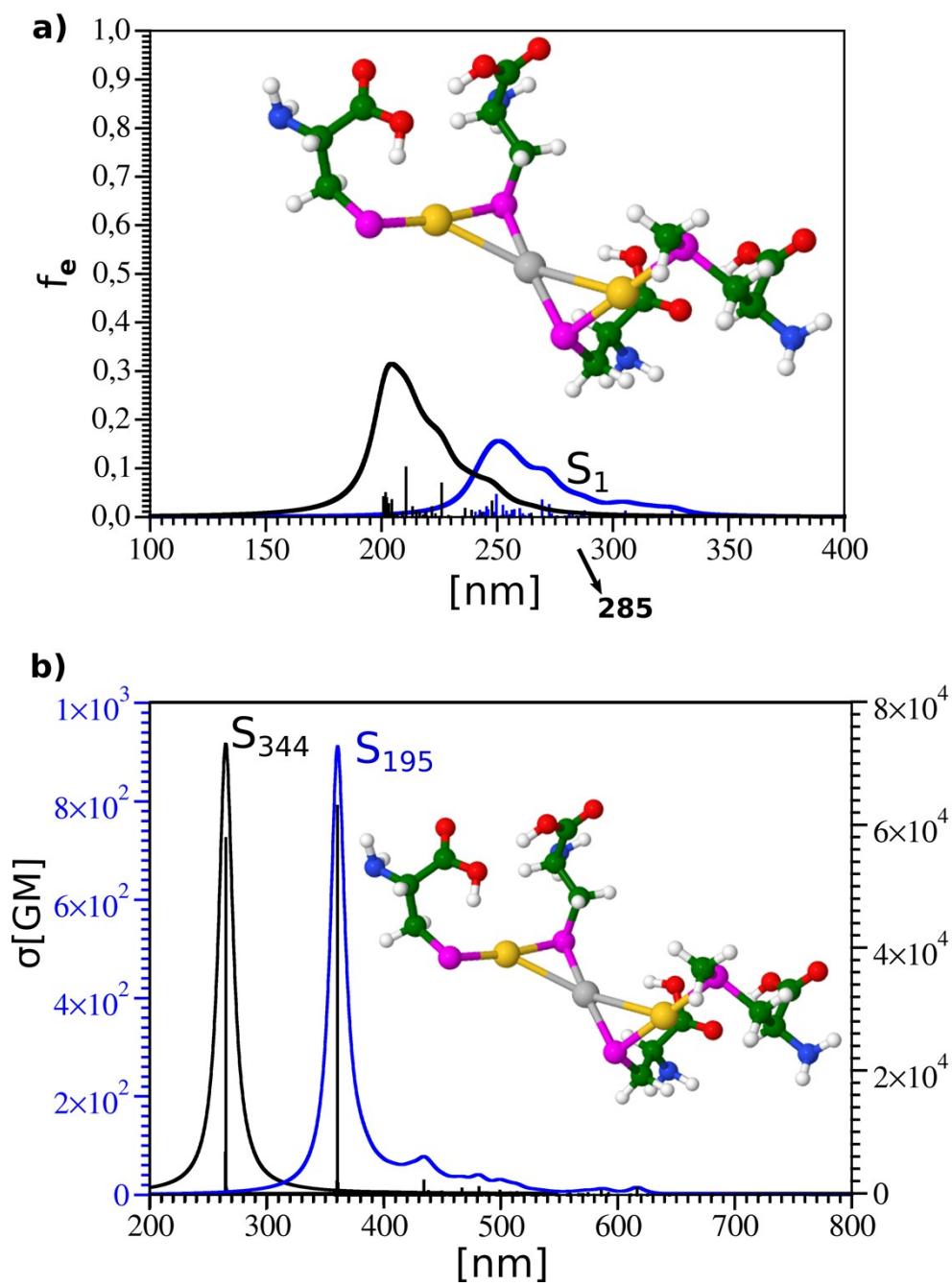


Figure S13: Comparison of TDDFT OPA (a) and TPA (b) spectra obtained with CAM-B3LYP (black) and B3LYP (blue) functionals for model system doped by Ag atom Au_2 -Ag-Cys₄-CH₃.

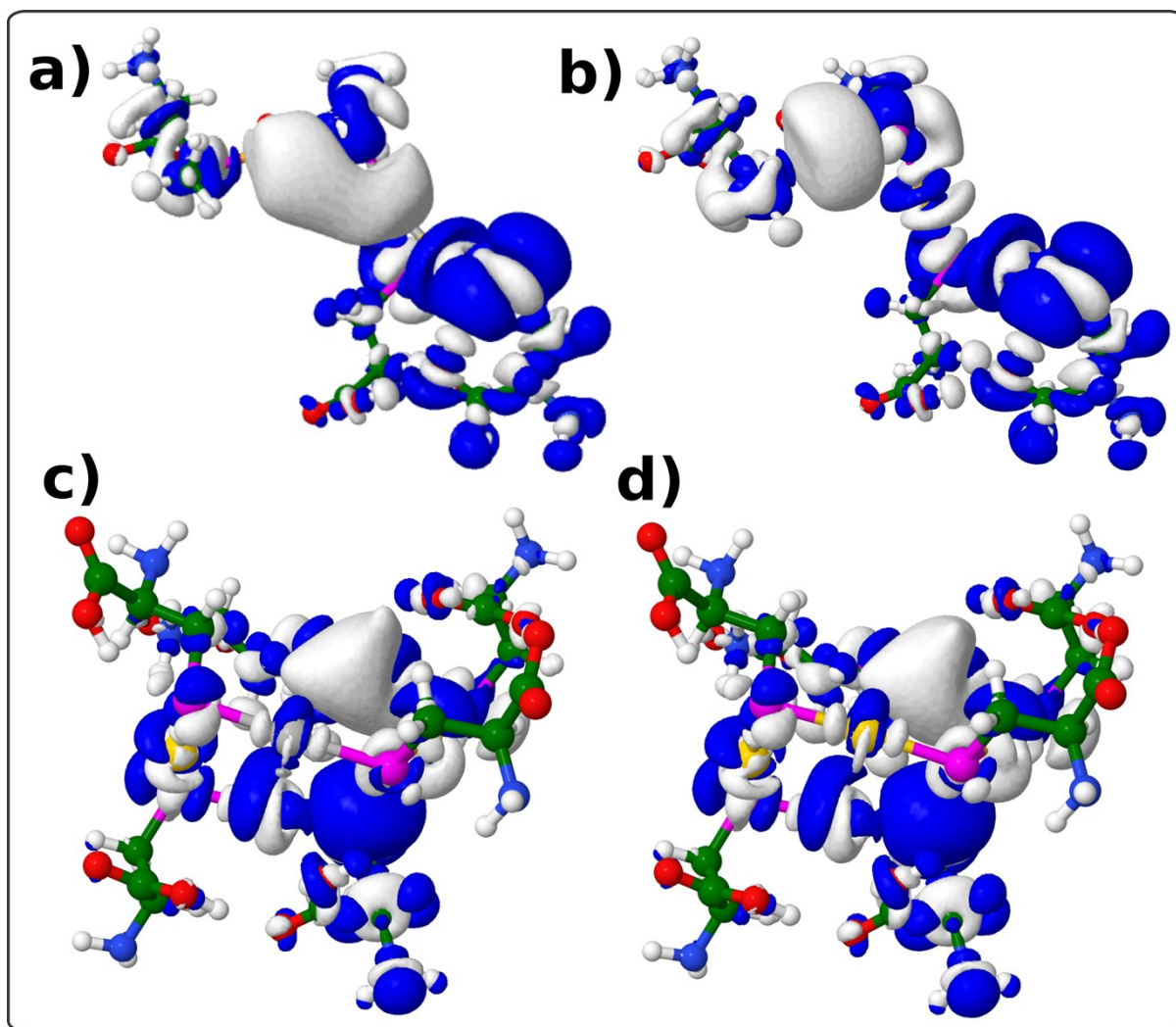


Figure S14: Electron density difference $\Delta\rho$ between electronic first excited state and ground state for a) $\text{Au}_2\text{-Ag-Cys}_4\text{-CH}_3$ and b) $\text{Au}_3\text{-Cys}_4\text{-CH}_3$ at 360 nm, c) $\text{Au}_4\text{-Ag-Cys}_6\text{-CH}_3$ at 378 nm and d) $\text{Au}_5\text{-Cys}_6\text{-CH}_3$ at 373 nm obtained using B3LYP (isovalue=0.001 a.u.). $\Delta\rho > 0$ (white), $\Delta\rho < 0$ (blue)